Eur Biophys J (2008) 38:121–125
DOI 10.1007/s00249-008-0366-0

BIOPHYSICS LETTER

Transport at the nanoscale: temperature dependence of ion conductance

**Catalin Chimerel · Liviu Movileanu ·
Soroosh Pezeshki · Mathias Winterhalter ·
Ulrich Kleinekathöfer**

Received: 1 July 2008 / Revised: 5 August 2008 / Accepted: 6 August 2008 / Published online: 23 August 2008

Abstract Temperature dependent ion conductance in nanopores is measured in a wide range of electrolyte concentrations and compared with molecular modeling. Single outer membrane protein F (OmpF) channels from *E. coli* are reconstituted into planar lipid bilayers. In qualitative agreement with the experimental data, applied-field molecular dynamics unraveled atomistic details of the ion transport. Comparing the temperature dependence of the channel conductance with that of the bulk conductivity in the range from 0 to 90°C revealed that at low salt concentrations the transport is mainly driven along the pore surface. Increasing the salt concentration saturates the surface charge transport and induces ion transport in the center of the nanopore. The confinement of the nanopore then favors the formation of ion pairs. Stepping up the temperature reduces the life time of the ion pairs and increases the channel conductance more than expected from the bulk behavior.

The exchange of ions and molecules between the interior and exterior of biological cells is mainly controlled by membrane proteins. One class of these membrane proteins forms aqueous channels and regulates the permeation of water soluble substances (Delcour 2003; Nikaido 2003). How nature controls these fluxes at the molecular level is currently an active field of research. A typical example of an aqueous nanochannel is the outer membrane protein F (OmpF), a trimeric porin which is present in the outer membrane of *E. coli* bacteria (Cowan et al. 1995) (Fig. 1). OmpF was the first membrane protein with available crystal structure and has been intensively investigated (see, for example, Alcaraz et al. 2004; Roux et al. 2004). The X-ray structure (Cowan et al. 1995) revealed that the shape of each monomer is approximately an asymmetric hourglass nanochannel with a nonuniform charge distribution at the surface. Each monomer forms a beta-barrel with eight turns at the periplasmic side of the channel and eight loops at the extracellular side. The L3 loop is particularly long and folds inside giving rise to a constriction zone of about 6 Å in diameter at about the middle of the lumen. The interior position of the L3 loop results in the main steric barrier and has a strong influence on the electrostatic interactions inside the nanopore. The predominantly negatively charge of the L3 loop contributes together with the positively charge on the opposite facing beta barrel to the formation of a strong transversal electric field. This electric field is able to orient water molecules in the constriction zone (Tieleman and Berendsen 1998) and to further determine specific ion pathways along the nanopore surface (Schirmer and Phale 1999; Phale et al. 2001; Im and Roux 2002b; Miedema et al. 2007). Through the interaction with the surface, the ions overcome the solvation barrier in the nanopore (Sansom et al. 1996; Im and Roux 2002b). A still open question is: what happens when the surface charge transport is saturated? As described, the mesoscopic dimension and the complexity of the channel render any exact model on the ion conductance difficult to formulate and thus impossible to solve analytically or numerically. Only approximative methods are presently

C. Chimerel · S. Pezeshki · M. Winterhalter ·
U. Kleinekathöfer (✉)
School of Engineering and Science, Jacobs University Bremen,
Campus Ring 1, 28759 Bremen, Germany
e-mail: u.kleinekathoefer@jacobs-university.de

L. Movileanu
Department of Physics, Syracuse University,
201 Physics Building, Syracuse, NY 13244-1130, USA

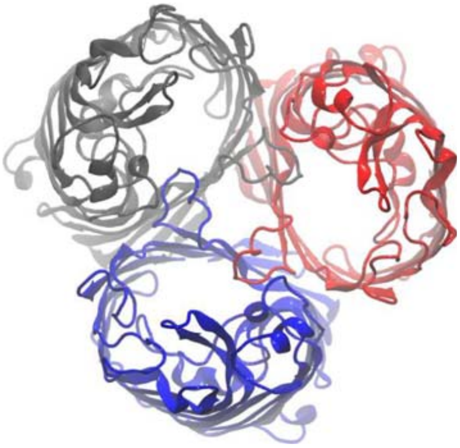

Fig. 1 Backbone structure of the OmpF trimer. Figure created using VMD (Humphrey et al. 1996)

available. A possible way to determine the qualitative behavior of the ion conductance is by solving the Poisson-Nernst-Planck equations with an appropriate charge distribution (Schuss et al. 2001). One step going towards particle-based theories of ion conductance are Brownian dynamics simulations (Schirmer and Phale 1999; Phale et al. 2001; Roux et al. 2004).

Earlier molecular dynamics (MD) simulations of OmpF have been performed (Tieleman and Berendsen 1998; Suenaga et al. 1998; Robertson and Tieleman 2002; Im and Roux 2002a, b; Danelon et al. 2003, 2006). Recent advances in computing capacity allow for large scale applied-field MD simulations and a direct calculation of the ion conductance. The simulations give access to atomic details of the transport mechanism through nanopores as has been shown for α-hemolysin (Aksimentiev and Schulten 2005) and MscS (Sotomayor et al. 2007). This approach is by far the most computational expensive method for calculating ion currents through a pore. However it yields novel information about the atomic details of the problem. Still there are restrictions to this method such as the non-polarizability and the temperature independence of standard force fields. In this letter we combine experimental data of OmpF conductance over a large scale of temperature and salt concentrations with MD simulations to get new insight into the ion transport mechanisms of nanochannels.

Electrophysiology allows high accuracy measurements of low ion currents generated by a transmembrane potential across nanopores. A single OmpF nanopore is embedded into an electric insulating lipid bilayer and connects two electrolyte solutions. When a voltage is applied across the lipid bilayer and implicitly across the nanopore a corresponding ion current is detected. Lipid bilayers are formed according to the method by Montal and Mueller (1972). A few details in the procedure need to be modified for a successful electrophysiology study on such a broad temperature range. The bilayer chamber and the peltier element used for temperature modification are previously described (Kang et al. 2005; Jung et al. 2006). A prepainting solution of 1% squalene in pentane is used. The lipid used has to remain in a single phase for an accurate determination of the ion transport through the pore. DPhPC (1,2-Diphytanoyl-sn-Glycero-3-Phosphatidylcholine) with a phase transition at 120°C is used (Lindsey et al. 1979; Kang et al. 2005). For keeping the pH constant at 7.5 over the studied temperature interval the 10 mM potassium phosphate buffer is suited (Kang et al. 2005). To improve the stability of the bilayer for high temperatures a 50–60 µm hole in the teflon film is needed. Ag/Cl electrodes were used and oil was added on the surface of the electrolyte to prohibit evaporation.

In Fig. 2 typical ion currents for a single trimeric OmpF channel in 1 M (molar) KCl are shown for a transmembrane voltage of 50 mV and different temperatures. As expected for bulk ion solution, increasing the temperature from 0 to 90°C increases the channel conductance. It is interesting to note that OmpF shows voltage dependent channel closure. The higher the voltage, the more gating occurs. Rising temperature enhances gating.

In order to understand the behavior of the ions inside the nanopore we analyze the temperature dependence of the nanopore conductance respectively the bulk conductivity at four different salt concentrations. In Fig. 3a, b the temperature dependent bulk conductivity and channel conductance are shown. The experimental errors are within the size of the symbols. A linear increase of both quantities with the temperature in the range of 0 to 90°C can be observed. However, the rates of increase for the bulk conductivity and for the nanopore conductance are different. Therefore the underlying mechanisms for ion transport

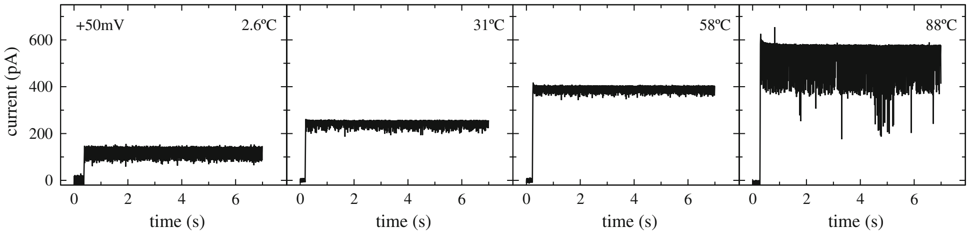

Fig. 2 Representative single channel traces obtained at different temperatures for wildtype OmpF in 1 M KCl solution at pH 7.5 and a transmembrane potential of 50 mV

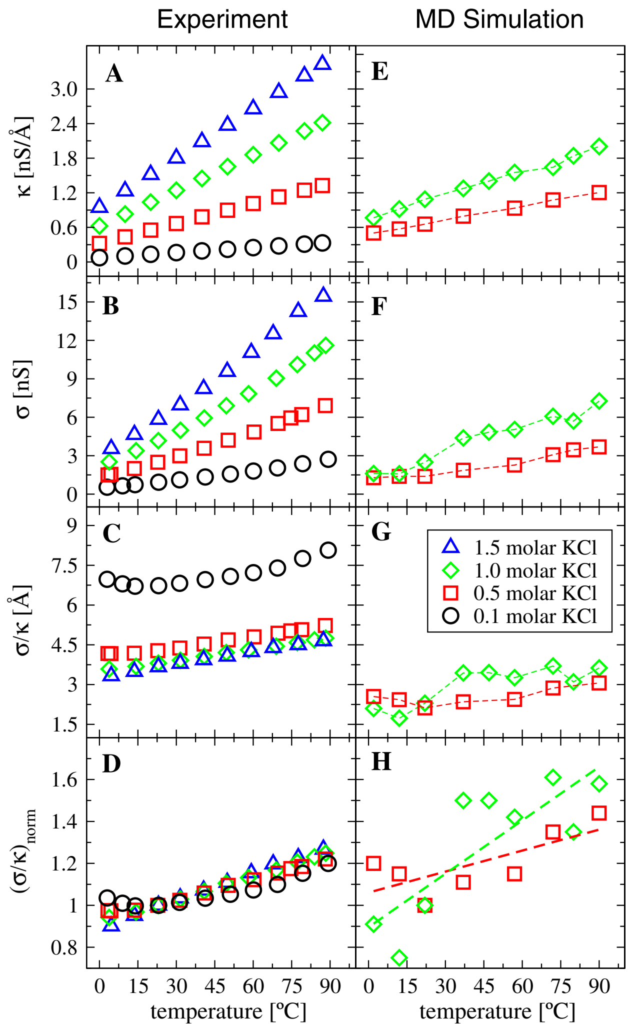

Fig. 3 Conductivity of the electrolyte and conductance of the OmpF nanopore as a function of temperature for KCl concentration varying from 0.1 to 1.5 M. Experimental results (50 mV applied across the membrane) are shown in the *left column*, results of the MD simulation (1 V applied across the membrane) in the *right column*. The *top row* shows the conductivity of the electrolyte, the *second row* the conductance of the OmpF trimer, the *third row* the ratio of OmpF conductance and bulk conductivity and the *lowest row* the same quantity but normalized at 23°C. The *dashed lines* in *panel H* represent linear fits

need to be further investigated. To make the differences between bulk and nanopore ion transport more visible, we plot in Fig. 3c the ratio of pore conductance and bulk conductivity versus temperature. The ratio is largest for 0.1 M KCl while the values for the 0.5 M concentration are much smaller. Going to even higher salt concentrations does change the ratio of conductance over conductivity only slightly. On the other hand increasing the temperature leads to an increase in the ratio conductance over conductivity as observed in Fig. 3c. In Fig. 3d the ratio of OmpF conductance and bulk conductivity is normalized at 23°C. The normalized ratio increases per 90°C by about 20% for a 0.1 M KCl and by about 30% for a 1.5 M KCl solution.

In the following we are going to describe the MD simulations and their results. The calculations were all performed using NAMD2 (Phillips et al. 2005) using the CHARMM27 (MacKerell et al. 1998) force field with the TIP3P water model (Jorgensen et al. 1983). The electrostatics is calculated using the partial-mesh Ewald method. First the system is equilibrated in a NPT setup and then, using a NVT ensemble, an electric field is applied in z direction. For the calculation of the ion current in the electrolyte and through the pore we used the method by Aksimentiev and Schulten (2005) given in (1), i.e., the current is determined using a discretized version of the z components of the velocity of all ions with charge q_i (Aksimentiev and Schulten 2005)

$$I(t) = \frac{1}{L_z} \sum_{i=1}^{N} q_i \frac{z_i(t + \Delta t) - z_i(t)}{\Delta t}. \qquad (1)$$

In the current study a Δt of 10 ps for evaluating this expression is sufficient. Using this method instead of counting the ions passing through a surface decreases the standard deviation (for one trajectory) by 2–3 orders of magnitude. The current is determined from single trajectories of roughly 10 ns length. A sampling over several trajectories and/or longer trajectories is certainly desirable but computationally extremely expensive. Therefore it is also not possible to give reliable error estimations. Especially for smaller voltages and/or concentrations the error becomes certainly not negligible.

In the first step we calculate the temperature dependence of the conductivity in 0.5 M and 1.0 M KCl solutions. The size of the system is a cube of approximately 40 Å side length. The results are shown in Fig. 3e. Also for the ion transport through the OmpF trimer all-atom MD simulations are performed. From the crystal structure 2OMF (Cowan et al. 1995) a trimer is formed and embedded into a POPE (1-Palmitoyl-2-Oleoyl-sn-Glycero-3-Phosphoethanolamine) membrane. First we used 112,035 atoms (side length of hexagon in x–y direction 69 Å and in z direction 75 Å) for the 1 M KCl solution and later on reduced the membrane patch leading to only 85,200 atoms (side length of hexagon in x–y direction 65 Å and in z direction 83 Å). The simulations with these different system sizes resulted in very similar results (within statistical errors). Therefore we used the smaller system size for 0.5 M KCl. The 1.0 (0.5) M KCl solution contained 388 (164) potassium and 358 (134) chlorine ions. Details of these simulations will be given elsewhere. The calculations are done with a time step of 1 fs since hydrogen bond restrictions lead to changes in the conductivity of up to 20%. The simulation time is roughly 10 ns per data point. As seen in Fig. 3f the agreement of the temperature dependence of the simulated and measured nanopore conductance is not perfect but reasonable. One has to clearly state that the experiments have been performed using a trans-membrane voltage of 50 mV and the calculations a voltage of 1 V. First tests (data not shown) indicate that the current–voltage characteristics is roughly linear for the experiments (in the range of -150 mV to $+150$ mV) and the simulations (in the range of -1 V to $+1$ V) at 0.5 M and 1 M KCl salt concentrations. Reducing the applied voltage (or the salt concentration) by a certain factor in the simulations leads to an increase of computing time by about the same factor shown in Fig. 3g is the theoretical result for the ratio of OmpF conductance to bulk conductivity. Compared to the experimental data the absolute values are smaller. But as observed during the experiments, the MD data show small differences between 0.5 and 1 M salt concentration. In Fig. 3h the normalized ratios of conductance and conductivity are shown. The agreement with experiment is only qualitative in the sense that the normalized ratio increases faster for higher salt concentrations than for smaller ones.

For most results shown the agreement between the experimental and theoretical results is reasonable though the normalized ratios conductance over conductivity certainly indicate the need for improvement beyond standard MD simulations. Nevertheless, this degree of agreement allows us to conclude on atomic details of the ion transport in nanopores. The ion binding to certain residues within the channel, has no clear dependence on temperature although at low temperatures there seems to be a prolonged binding time. The number of ions inside the channel is basically temperature independent as can be seen in Fig. 5. As our and previous simulations (Schirmer and Phale 1999; Im and Roux 2002b) show, positive and negative ions have distinct pathways on the surface of the constriction zone, i.e., the two ion types are separated. For low ion concentrations, such as 0.1 M KCl, mainly potassium ions are in the channel and these are close to the channel surfaces and none in the middle of the channel whereas for 1 M KCl the surface transport is saturated and the still distinct ion densities are extended towards the center of the channel. This enlarges the possibility for ion pair formation.

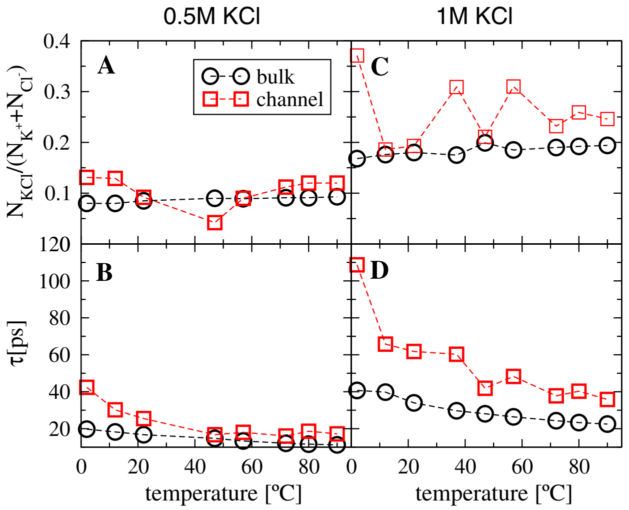

Fig. 4 Fraction of paired ions (*top row*) and life time of the ion pairs (*lower row*) for 0.5 M (*left column*) and 1.0 M KCl solutions (*right column*) from the MD simulations

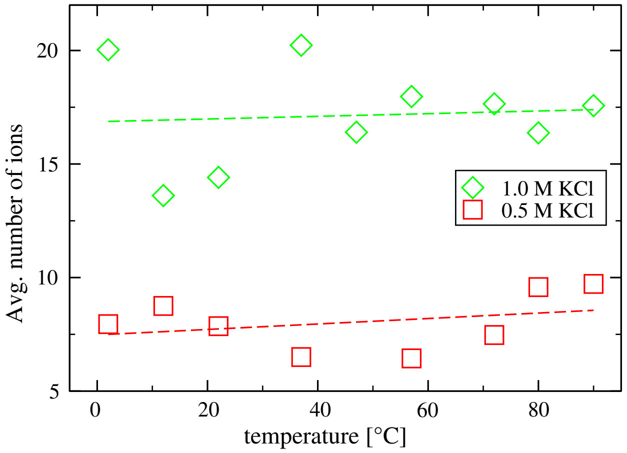

Fig. 5 Temperature dependence of the number of ions in the OmpF channel. The *lines* show linear fits of the individual temperature data points

Due to the confinement the ion pairing may influence the conductance. The atomistic details of the MD simulations allow to investigate this further. Ions of opposite charge being at distances below 4.1 Å are counted as pairs. To quantify their concentration inside the channel a region of around 12 Å length in the constriction zone was analyzed. Figure 4a, c shows the increase in ion pairs for increasing ion concentrations. At 0.5 M the number of pairs in the channel is about the same than in the bulk whereas at 1 M KCl their concentration roughly doubles in the bulk and triples in the channel. The number of ion pairs seems to be rather temperature independent (see Fig. 4a, c) whereas, the lifetime decreases with increasing temperature as shown in Fig. 4b, d. We may hypothesize inasmuch this effect may contribute to the channel conductance. Confinement promotes ion pair formation, which in turn has an effect on ion channel conductance. At concentrations of 0.5 M or less the number of ion pairs in the channel is the same than in the bulk and no effect on conductance is expected. However, at higher ion concentrations more ions are trapped in pairs inside the channel than in the bulk. The life-time of the pairs decreases with increasing temperature and this will lead to faster transport of ions with a different temperature dependence in the channel than in the bulk. A more quantitative analysis of this contribution to channel conductance may be introduced into basic models of ion transport.

In conclusion, the combination of experiment with modeling gives access to atomic details of the ion transport. The temperature study allows to understand and specifically vary various aspects of ion transport. Mesoscopic channels in the range of about 1 nm in diameter show a qualitative similar behavior to the bulk for high salt concentrations and start to deviate from the bulk behavior at low salt concentrations. It was shown that the relative increase in conductance with temperature is larger in the pore than in bulk. Using applied-field MD we were able to show that there is an enhanced number of ion pairs in the channel with decreasing lifetime at higher temperatures. From this atomic detail it was proposed that this higher probability of breaking and making ion pairs at larger temperatures does lead to an increase in charge carriers which in turn leads to an increase in conductance. Both surface conductance and ion pairing contribute to ion transport and are modulated by the structure of the mesoscopic channel. This study shows that one needs to look at atomic level to understand differences in bulk and channel conductance. It opens certainly a large field of investigations for natural and artificial pores and their design to fulfill certain properties.

Acknowledgments M.W. acknowledge financial support through MRTN-CT-2005-019335 (Translocation) as well as L.M. from Syracuse University start-up funds and the US National Science Foundation Grant DMR-706517. Additionally, we thank Aiping Zhu and Luminita Damian for their help during the preliminary stage of this work.

References

Aksimentiev A, Schulten K (2005) Imaging alpha-hemolysin with molecular dynamics: ionic conductance, osmotic permeability, and the electrostatic potential map. Biophys J 88:3745–3751

Alcaraz A, Nestorovich EM, Aguilella-Arzo M, Aguilella VM, Bezrukov SM (2004) Salting out the ionic selectivity of a wide channel: the asymmetry of OmpF. Biophys J 87:943–947

Cowan SW, Garavito RM, Jansonius JN, Jenkins JA, Karlsson R, Konig N, Pai EF, Pauptit RA, Rizkallah PJ, Rosenbusch JP et al (1995) The structure of OmpF porin in a tetragonal crystal form. Structure 3:1041–1050

Danelon C, Suenaga A, Winterhalter M, Yamato I (2003) Molecular origin of the cation selectivity in ompf porin: single channel conductances vs. free energy calculation. Biophys Chem 104:591–603

Danelon C, Nestorovich EM, Winterhalter M, Ceccarelli M, Bezrukov SM (2006) Interaction of zwitterionic penicillins with the OmpF channel facilitates their translocation. Biophys J 90:1617–1617

Delcour AH (2003) Solute uptake through general porins. Front Biosci 8:d1055–d1071

Humphrey WF, Dalke A, Schulten K (1996) VMD—visual molecular dynamics. J Mol Graph 14:33–38

Im W, Roux B (2002a) Ion permeation and selectivity of OmpF porin: a theoretical study based on molecular dynamics, Brownian dynamics, and continuum electrodiffusion theory. J Mol Biol 322:851–859

Im W, Roux B (2002b) Ions and counterions in a biological channel: a molecular dynamics simulation of OmpF porin from Escherichia coli in an explicit membrane with 1 M KCl aqueous salt solution. J Mol Biol 319:1177–1197

Jorgensen WL, Chandrasekhar J, Madura JD, Impey RW, Klein ML (1983) Comparison of simple potential functions for simulating liquid water. J Chem Phys 79:926–935

Jung Y, Bayley H, Movileanu L (2006) Temperature-responsive protein pores. J Am Chem Soc 128:15332–15340

Kang XF, Gu L-Q, Cheley S, Bayley H (2005) Single protein pores containing molecular adapters at high temperatures. Angew Chem Int Ed Engl 44:1495–1499

Lindsey H, Petersen NO, Chan SI (1979) Physicochemical characterization of 1,2-diphytanoyl-sn-glycero-3-phosphocholine in model membrane systems. Biochim Biophys Acta 555:147–167

MacKerell A, Bashford D, Bellott M, Dunbrack R, Evanseck J, Field M, Fischer S, Gao J, Guo H, Ha S, Joseph-McCarthy D, Kuchnir L, Kuczera K, Lau F, Mattos C, Michnick S, Ngo T, Nguyen D, Prodhom B, Reiher W, Roux B, Schlenkrich M, Smith J, Stote R, Straub J, Watanabe M, Wiorkiewicz-Kuczera J, Yin D, Karplus M (1998) All-atom empirical potential for molecular modeling and dynamics studies of proteins. J Phys Chem B 102:3586–3616

Miedema H, Vrouenraets M, Wierenga J, Meijberg W, Robillard G, Eisenberg B (2007) A biological porin engineered into a molecular, nanofluidic diode. Nano Lett 7:2886–2891

Montal M, Mueller P (1972) Formation of bimolecular membranes from lipid monolayers and a study of their electrical properties. Proc Natl Acad Sci USA 69:3561–3566

Nikaido H (2003) Molecular basis of bacterial outer membrane permeability revisited. Microbiol Mol Biol Rev 67:593–656

Phale PS, Philippsen A, Widmer C, Phale VP, Rosenbusch JP, Schirmer T (2001) Role of charged residues at the OmpF porin channel constriction probed by mutagenesis and simulation. Biochemistry 40:6319–6325

Phillips JC, Braun R, Wang W, Gumbart J, Tajkhorshid E, Villa E, Chipot C, Skeel RD, Kale L, Schulten K (2005) Scalable molecular dynamics with NAMD. J Comput Chem 26:1781–1782

Robertson KM, Tieleman DP (2002) Orientation and interactions of dipolar molecules during transport through OmpF porin. FEBS Lett 528:53–57

Roux B, Allen T, Berneche S, Im W (2004) Theoretical and computational models of biological ion channels. Q Rev Biophys 37:15–103

Sansom MS, Kerr ID, Breed J, Sankararamakrishnan R (1996) Water in channel-like cavities: structure and dynamics. Biophys J 70:693–702

Schirmer T, Phale PS (1999) Brownian dynamics simulation of ion flow through porin channels. J Mol Biol 294:1159–1167

Schuss Z, Nadler B, Eisenberg RS (2001) Derivation of poisson and nernst-planck equations in a bath and channel from a molecular model. Phys Rev E 64:036116

Sotomayor M, Vasquez V, Perozo E, Schulten K (2007) Ion conduction through MscS as determined by electrophysiology and simulation. Biophys J 92:886–902

Suenaga A, Komeiji Y, Uebayasi M, Meguro T, Saito M, Yamato I (1998) Computational observation of an ion permeation through a channel protein. Biosci Rep 18:39–48

Tieleman DP, Berendsen HJ (1998) A molecular dynamics study of the pores formed by Escherichia coli OmpF porin in a fully hydrated palmitoyloleoylphosphatidylcholine bilayer. Biophys J 74:2786–2791